Journal of Non-Crystalline Solids 147&148 (1992) 375–381
North-Holland

JOURNAL OF
NON-CRYSTALLINE SOLIDS

Drying process in the formation of sol–gel-derived TiO_2 ceramic membrane

Krishnankutty-Nair P. Kumar, V.T. Zaspalis, K. Keizer and A.J. Burggraaf

Laboratory for Inorganic Chemistry Materials Science and Catalysis, Faculty of Chemical Technology, University of Twente, 7500 AE Enschede, The Netherlands

Accurate drying data for thin titania gel layers dried at 40°C and 20% relative humidity (RH) are given. The drying rate versus free moisture content diagram should show three regions as predicted by the classical drying theory. They are the constant rate period, the first falling rate period and the second falling rate period. The second falling rate period was not observed in the present case, because at 40°C and 20% RH the equilibrium moisture content will be enough to provide a continuous fluid network in the gel. The total drying time in the falling rate period increases with layer thickness. The drying mechanism in the first falling rate period was identified as capillary flow.

1. Introduction

Ceramic membranes are a new generation of multi-functional engineering ceramic systems applied for water desalination, ultrafiltration and separation of gas mixtures. They are also projected as potential candidates for catalytic active and carrier membranes. The initial stage in the formation of ceramic membranes consists of preparation of a stable sol and gelling it on a porous support by a dipping procedure [1]. Most published works have concentrated on the properties and applications of membranes. Few have dealt with the formation process. Burggraaf and co-workers [1,2] have shown that the formation of a gel layer on a porous support is by a slip casting mechanism. The present work is carried out with a view to understand the drying and gelling phenomena and the accompanied nanostructural evolution of hydrogel layers supported on both porous and nonporous supports.

Drying is one of the most crucial steps in the formation of ceramic membranes because membranes tend to crack during the process, and avoiding cracking requires very slow drying rates. Early analysis [3] of isothermal drying was based on Fick's second law in which shrinkage was taken into account by introducing appropriate diffusion coefficients. An alternative approach to drying phenomena based on capillarity was suggested by Coming and Sherwood [4] and Hougen et al. [5] to show the limitation of the diffusion model. A useful summary of the drying literature is given by Simpkins et al. [6].

One of the first attempts to understand the drying of ceramic green bodies was by Cooper [7]. He analyzed drying of clay bodies based on a diffusion model. The first attempt to study the drying of gels was made by Zarzycki [8]. He suggested a modification to Cooper's model by introducing a global term called 'moisture stress'. Moisture stress can be considered as equivalent to the work done in removing a unit mass of water from the water–gel system to a free water surface at the same temperature and head. Thermodynamically, it is partial Gibb's free energy of water in the system. The term takes into account the contributions from capillary pressure, osmotic pressure and disjoining pressure (electrostatic). Drying due to capillarity applies to all water in excess of the equilibrium moisture content at atmospheric saturation. However this model does not account for the fact that fluid in a porous body flows according to Darcy's law [9]. Also, the

model does not consider the mechanical properties of the gel. Recently Scherer [9] has proposed a quantitative model for the drying behaviour of gels based on a combined capillary flow and diffusion mechanism. Experimental results on drying of thin sol–gel layers are very rare. Experimental results on drying of alumina gels were reported by Dwivedi [10]. The purpose of this work is to study the drying and the accompanied processes such as stress development [11] in this sol–gel ceramic membrane layers. In the present paper, we report the results of the systematic investigation on the drying behaviour of titania gel layers. These data were used to identify the mechanism of drying during the formation of supported ceramic membranes. This knowledge is necessary to interpret the results of stress measurement during drying [11].

2. Theory of drying

When a piece of gel is dried, in the first stage of drying, the volume shrinkage will be equal to the volume of water lost by evaporation. This will keep the fluid meniscus at the surface of the gel body as shown in fig. 1(a). This stage will continue till the solid skeleton attains certain strength. In this situation, the volume shrinkage rate will no longer maintain the fluid meniscus at the surface; the liquid will try to flow to the surface of the gel to avoid the more energetic solid/vapour interface (fig. 1(b)). This is the first falling rate period. This situation will continue until the flow from the interior is enough to balance the evaporation rate. In the last stage of drying, called the second falling rate period, the funicular distribution of water inside the pores will become pendular. Now the liquid transport is only by diffusion of vapour from the interior (fig. 1(d)). An excellent review on drying of gels has been given by Scherer [9].

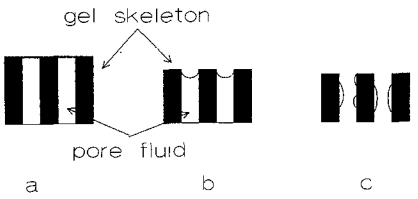

Fig. 1. Three different stages of drying: (a) constant rate period, (b) first falling rate period and (c) second falling rate period.

3. Experimental

Drying experiments were carried out in a climate chamber (Heraeus VTRK 300). Weight loss versus time data of this titania sol–gel drying layers were collected at different temperatures and relative humidities. In the actual membrane formation process, the weight of membrane precursor (hydrogel layer on the porous support just after dipping) is very small compared with the weight of the support. So the absolute amount of water present in the hydrogel layer will be in the order of few milligrams. This will make the drying experiment with the support/hydrogel layer system practically impossible. To avoid this difficulty, all the drying experiments were performed by pouring a dilute (0.3 mol) TiO_2 sol on a glass petri dish. Weight change with time was measured very accurately by using a Mettler microbalance and the data is directly downloaded to a PC. The weight of the drying gel was collected every 5 min until the weight remained constant. This is automatically done by the balance. Experiments were carried out with varying amounts of starting sol to get drying diagrams for gels with different dried thicknesses. Titania sol was prepared from titanium iso-propoxide. Preparation details are given in ref. [2].

4. Results

The drying experiments described above are different from the actual membrane drying in the following ways. (1) Water present in the pores of the support will interfere with the drying and stress relaxation behaviour because water inside the pores of the support will act as reservoirs and thereby extends the first stage of drying. (2) Interface bonding between glass and the gel layer is different from that of the support (porous Alu-

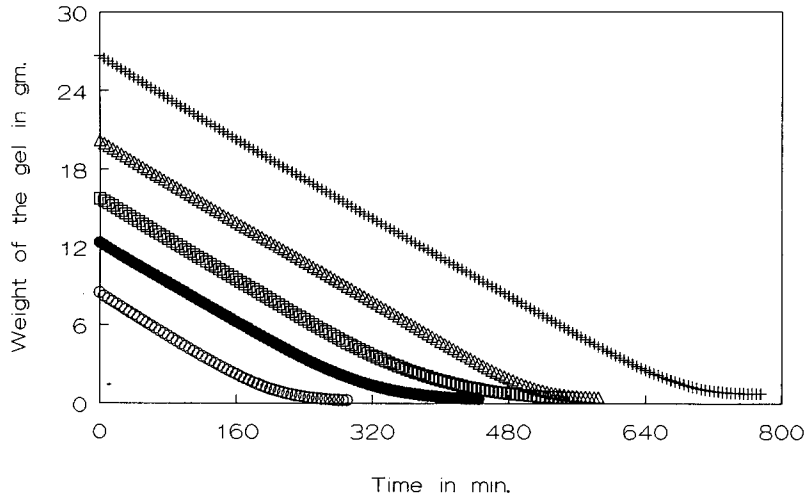

Fig. 2. The weight loss versus drying time data for supported titania gel layers dried at 40°C and 20% relative humidity, +, 60 μm; △, 46 μm; □, 35 μm, ●, 25 μm; ○, 17 μm.

mina) and gel layer. Even though in many cases membranes showed a tendency to delaminate from the glass support after drying, for all practical purposes glass/membrane system can be considered as supported membrane at least during drying. (3) In the model experiment, thickness of the dried layer is always > 10 μm, whereas the thickness of the actual supported membrane layer after drying is about 2–6 μm. However, it is assumed that in both the cases drying occurs only from the top surface.

Figure 2 shows the weight loss versus time data of titania gel layers of different dried thickness dried at 40°C and 20% relative humidity (RH). The data are presented without statistical smoothing. We can clearly see that, unlike the reported drying data [10], there is practically no scatter from the smooth centre line. The weight

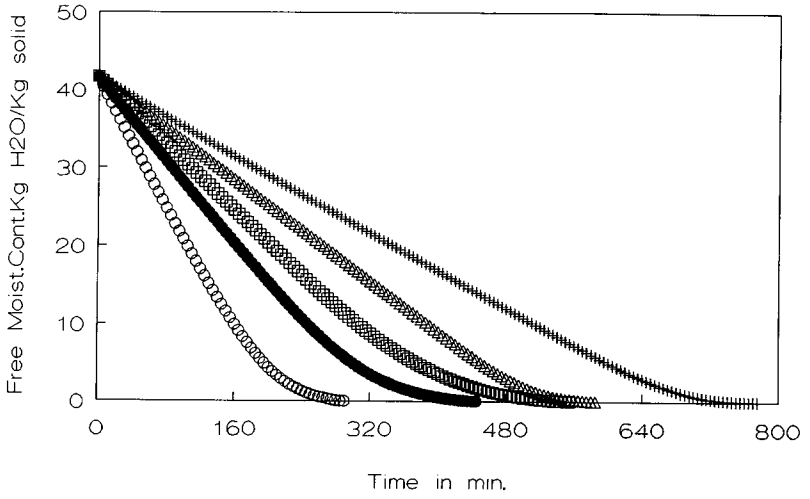

Fig. 3. Diagram showing the change of free moisture content with time. +, 60 μm; △, 46 μm; □, 35 μm; ●, 25 μm; ○, 17 μm.

loss versus time data represented in fig. 2 can be converted into a more useful form. It can be recalculated into free moisture content versus time form. Free moisture content of a wet gel is the amount of water which is present in excess of the equilibrium moisture content at the given temperature and relative humidity. If W_t is the total weight of the wet gel (water + dry solid) and W_s is the weight of the dry solid content, then the fraction of water present at time, t, is given by [12]

$$X_t = (W_t - W_s)/W_s, \quad (1)$$

and the fraction of water present after drying at the given drying condition is given by

$$X_e = (W_e - W_s)/W_s, \quad (2)$$

where W_e is the weight of gel after drying at the

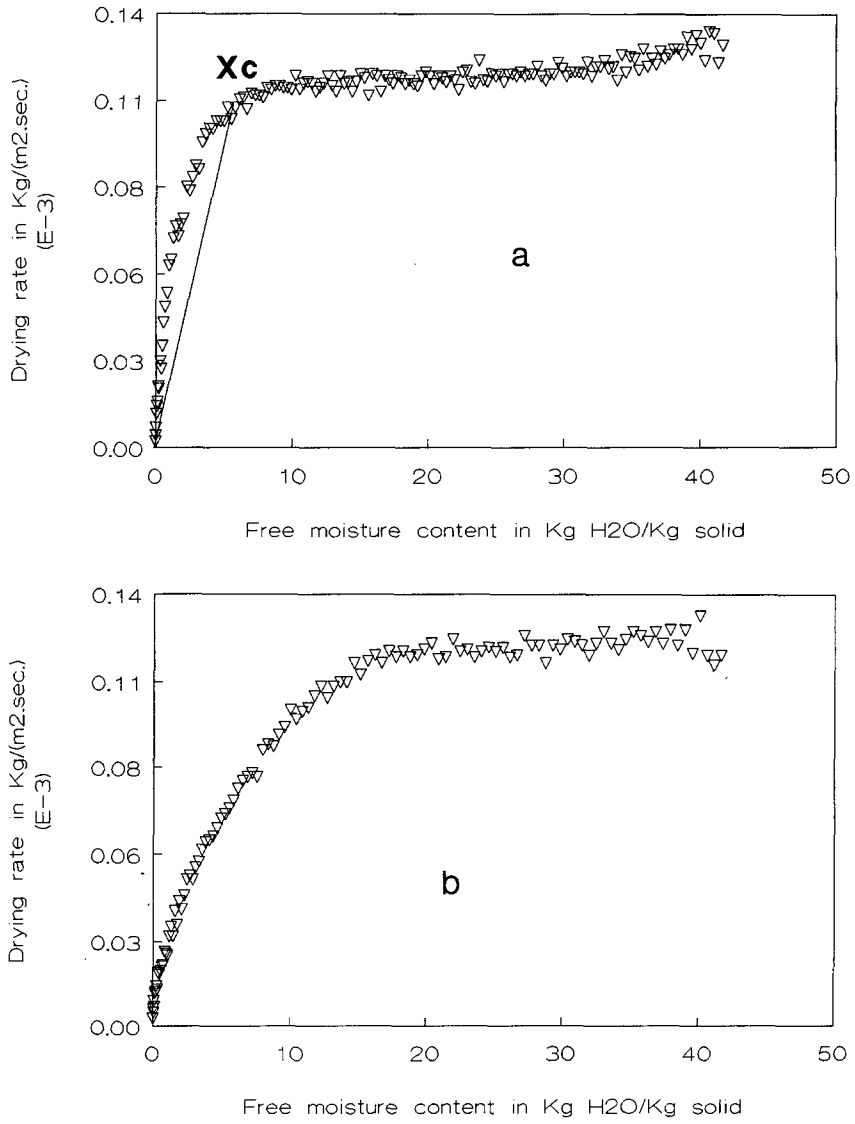

Fig. 4. Typical drying rate diagrams for titania gel layers of (a) 60 μm and (b) 35 μm thickness, dried at 40°C and 20% relative humidity.

set condition. From X_t and X_e, the free moisture content, X, can be calculated:

$$X = X_t - X_e. \quad (3)$$

Substituting the values of X_t and X_e from eqs. (1) and (2) in eq. (3), we obtain the expression for the free moisture content:

$$X = (W_t - W_e)/W_s. \quad (4)$$

Using eq. (4), the data presented in fig. 2 are recalculated and plotted as free moisture content, X, versus time diagram and presented in fig. 3. It can be noted from fig. 3 that the initial free moisture contents for all the experiments were the same irrespective of the layer thickness: it was about 42 (kg of water/kg solid). In the case of the gel layer with 60 μm thickness, the initial straight line portion extends up to about 540 min, representing the constant rate period of drying (CRP). This is about 70% of the total drying time in this case. The 46 μm thick membrane also shows similar behaviour. When the thickness decreases to about 35 μm, the transition from the CRP becomes less sharp compared with the thicker membranes. Moreover, the falling rate period starts after about 50% of the total drying time for the case of thinner membranes (see thicknesses $\leqslant 35$ μm).

Drying rate curves can be obtained using graphical differentiation by drawing tangents at every point in the free moisture versus time curve given in fig. 3. Analytically, drying rate, R, can be calculated as

$$R = -(W_s/A)\, dX/dt, \quad (5)$$

where A is the area available for drying. In the present case, A is about 5.28×10^{-3} m^2.

5. Discussion

Drying rates were calculated using the eq. (5) and presented in fig. 4. Figures 4(a) and (b) represent two typical drying diagram (drying rate versus free moisture) of titania gel layer of 60 and 35 μm, respectively, dried at 40°C and 20% relative humidity. The straight line portions perpendicular to the drying rate axis represent the constant rate period of drying. At this stage, the drying takes place from the water layer in the surface of the gel and there is no fluid meniscus. According to the classical drying theory, the drying rate at this stage corresponds to the rate of evaporation of the water from a free water surface. This prediction is in fact not in good agreement with the experimental results. The water evaporation rate at 40°C and 20% relative humidity was found to be about 1.5×10^{-4} kg/(m^2 s) whereas the drying rate in the constant rate period for the titania gel layer is about 1.2×10^{-4} kg/(cm^2 s) which is about 20% less than the value for pure water. This difference can probably be due to the fact that the pore fluid is not pure water, but a dilute solution of water and a higher alcohol. In the present case it is isopropyl alcohol. Moreover, the effective drying area available in the constant rate period may be little less than the actual area. In all drying experiments, the drying rate was slightly higher in the beginning of the CRP. This can be clearly seen in fig. 4(a). This is because at the beginning of drying the surface temperature of the gel is higher than the wet bulb, T_w, temperature, which is about 22.1°C at 40°C and 20% RH. When drying progresses, the gel surface will attain the wet bulb temperature and then the drying rate will remain constant throughout the CRP.

The changing over from CRP to falling rate period is relatively sharp in the case of the thick gel layer (fig. 4(a)). For thin layers (35 μm), we observe a smooth transition from CRP to falling rate period (fig 4(b)). At this stage, the reason for this behaviour is not understood properly. A probable explanation may be that the thinner layers may have more open network structure. When the layer thickness increases, the support constraint will have less and less influence on the overall layer. Moreover densification and rearrangement due to shearing is easier with thicker layers compared with the thinner ones.

The constant rate period starts when the volume shrinkage rate of the gel network can no longer cop-up the volume evaporation rate of the pore fluid [9]. In this stage, the mass transport is predicted to be through a capillary flow mechanism [9]. The falling rate period can be approxi-

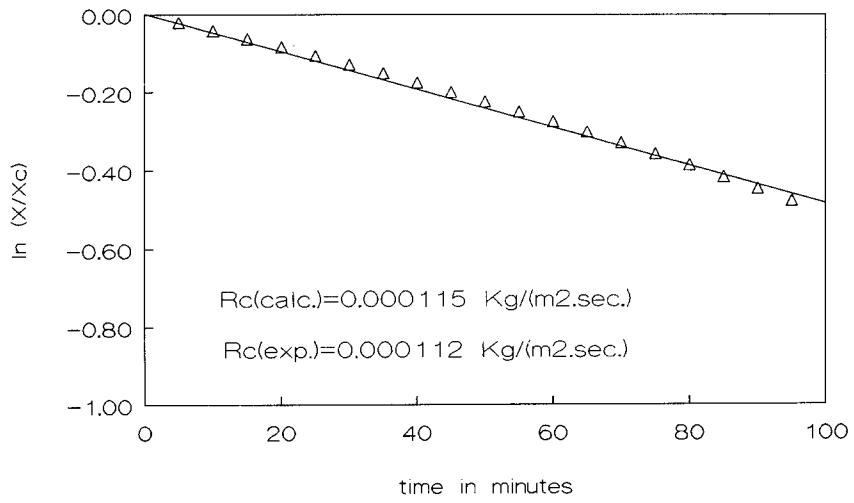

Fig. 5. $\ln(X/X_c)$ versus time plot of a gel layer of 60 μm thickness dried at 40°C and 20% RH, △, experimental points; ———, best fit line.

mated to a straight line drawn from zero moisture content to the critical moisture content, X_c. Critical moisture content is the free moisture present in the gel at the changing over from CRP to falling rate period. Drying rate at this stage can approximately be represented as

$$R = kX \tag{6}$$

where k is a constant, which is equal to R_c/X_c; R_c is the drying rate at CRP. Combining eqs. (5) and (6) and integrating for time, we obtain

$$t = (W_s X_c/AR_c)\ln(X_c/X). \tag{7}$$

If the mechanism is in fact capillary flow, then the slope of the best fit line on the time versus X/X_c data should be equal to $(W_s X_c/AR_c)$. From this value, the drying rate at CRP can be calculated and compared with the experimental re-

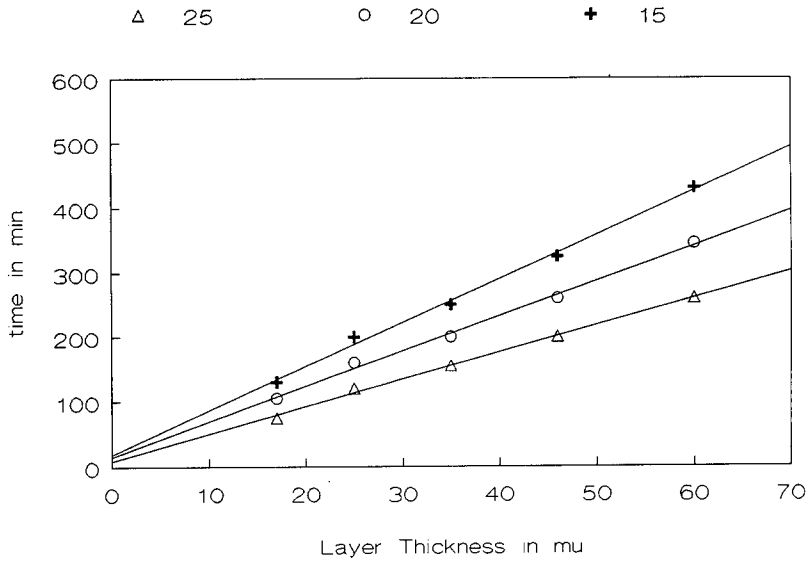

Fig. 6. Diagram showing the time required to reach a given level of free moisture content for membranes of different thickness dried at 40°C and 20% RH, △, 25; ○, 20; +, 15.

sults. A plot of time versus X/X_c is given in fig. 5. The R_c value calculated from fig. 5 is in good agreement with the experimental value of R_c. Therefore we have concluded that the flow mechanism in the first falling rate period is in fact through capillary flow.

The time required to attain a given level of free moisture content in the CRP as a function of layer thickness is presented in fig. 6. The numbers in the legends represent the free moisture levels reached. As expected, the time required to reach a given level of moisture content in the CRP will increase with layer thickness. These diagrams can be used for predicting the free moisture content levels in CRP for titania gel layers drying at a given condition.

6. Conclusion

Drying data of sol–gel-derived titania thin layers are reported. In the drying condition studied the drying rate versus free moisture content diagram showed the constant rate period and the first falling rate period as predicted by classical drying theory. The second falling rate period was not observed because at 40°C and 20% RH the equilibrium moisture content will be enough to provide a continuous fluid network in the gel. The total drying time in the constant rate period increases with layer thickness. The drying mechanism in the first falling rate period was identified as capillary flow. Work is in progress to elucidate the mechanism of fluid transport in the second falling rate period.

References

[1] A.F.M. Leenaars, K. Keizer and A.J. Burgraaf, J. Mater. Sci. 19 (1984) 1077.
[2] V.T. Zaspalis, W. van Praag, K. Keizer, J.R.H. Ross and A.J. Burggraaf, J. Mater. Sci. 27 (1992) 1023.
[3] T.K. Sherwood, Ind. Eng. Chem. 21 (1929) 12.
[4] E.W. Coming and T.K. Sherwood, Ind. Eng. Chem. 26 (1934) 1096.
[5] O.A. Hougen, H.J. McCauley and W.R. Marshall, Trans. Am. Inst. Chem. Eng. 36 (1940) 183.
[6] P.G. Simpkins, D.W. Johnson Jr. and D.A. Fleming, J. Am. Ceram. Soc. 72 (1989) 1816.
[7] A.R. Cooper, in: Ceramic Processing Before Firing, ed. G. Onida and L. Hench (Wiley, New York, 1978) p. 216.
[8] J. Zarzycki, in: Glass: Science and Technology, ed. D.R. Uhlmann and N.J. Kreidl (Academic Press, Orlando, FL, 1984) p. 209.
[9] G.W. Scherer, J. Am. Ceram. Soc. 73 (1990) 3.
[10] R.K. Dwivedi, J. Mater. Sci. Lett. 5 (1986) 373.
[11] Krishnankutty-Nair P. Kumar, V.T. Zaspalis, K. Keizer and A.J. Burggraaf, 'Stress development during drying of sol–gel-derived ceramic membranes', presented at 6th Int. Workshop on Glasses and Ceramics from Gels, 1991.
[12] C.J. Geankoplis, Transport Processes and Unit Operations (Allyn and Bacon, MA, USA, 1983).